Sindh Univ. Res. Jour. (Sci. Ser.) Vol.47 (2) 371-376 (2015)

SINDH UNIVERSITY RESEARCH JOURNAL (SCIENCE SERIES)

Modelling and Simulation of Fluid Flow between Two Discs Rotating at Different Direction

A. F. ABBASI, S. A. SHAH* M. S. JUMANI** B-UL-H, BALOCH***

Department of Mechanical Engineering Mehran University of Engineering and Technology, Jamshoro, Sindh, Pakistan. (Corresponding Author)

Received 27th May 2014 and Revised 8th December 2014

Abstract: *This paper presents the modelling and simulation work for the fluid flow between two discs rotating in opposite direction, commonly known as the contra rotating discs system. These systems of the discs may apply to future generation engines of high rotating speeds* (*Gan et al., 1995). Two turbulence models, the low Reynolds number k-ε model and low Reynolds number second moment closure with finite-difference approach have been implicated to obtain the numerical solution. All the simulation work has been carried out according the experimental work of (Chen et al., 1997) for the range of Reynolds number and mass flow rate* $Re_\Theta = 1.14x10^6 \leq 1.19x10^6$ *and* $C_w = 4026 \leq 9351$*respectivily , at the disc speed ratio,* Γ*=-1. Simulated results of radial and tangential velocity profiles at different radial location showed fine agreement with the measurements. The computed moment coefficients of both the models illustrated the similar trend of variation in accordance to the mass flow rate and rotational. speed of the discs*

Keywords Turbomachinery, Contra-rotating disc flows, Low Reynolds number Second moment closure

1. INTRODUCTION

Two discs rotating in opposite direction have the great scope of applicability in the ultra-high-bypass-ratio engines to drive the contra-rotating fan blades as proposed by (Gan et al.,1994). This system of discs may waved-off the use of nozzle guide vane blades and decrease the weight and size of the engine. Review of previous research work mostly focused on the various turbulence models and their application to rotor-stator and corotating disc systems however, less attention has been given to the contra rotating disc flow system and the application of Reynolds stress model. The Reynolds Stress model is based on the suggestion of (Morse,1988) , (Lai and So,1990) and (Memon *et al.,* 1995) Recently, (Abbasi, 2013) has used Reynolds Stress model for rotating disc systems. (Rémi Manceau, 2014) further investigated the near wall turbulence mechanism and made some modifications in the Reynolds stress model and validated the simulated results with the DNS database of channel flow results. (Kilic *et al.,* 1994) presented the computational and experimental study of contra-rotating discs system, for range disc speed ratios $-1 \leq \Gamma \leq 0$ .They mentioned that for pure contra rotating case $\Gamma = -1$, the laminar flow was formed on both sides of the discs, however, turbulent flow was formed in the midplane in reverse direction. Result of that two cell structures were formed between the discs. At the intermediate values of disc speed ratios (Γ), the size of cells decreased monotonically and stagnated at the slower disc. Later on same authors (Kilic *et al.,* 1995 and 2003) investigated the fluid flow behaviour for higher rotational speed of $Re_\Theta = 10^6$. The numerical studies of (Hill and Ball, 1997 and 1999) also demonstrated the significant effects of disc speed ratio on the flow structure. (Soong *et al.,* 2003) investigated flow structure between two co-axial discs rotated independently through the injection of smoke. Their experimental studies confirmed the basic flow structures which were presented in the previous research work. In the present work two turbulence models, the low Reynolds number k-ε model and low Reynolds number second moment closure have been used to predict the fluid flow behaviour between two discs rotating at different speeds. In this state of art system, two discs are rotating with certain angular velocity (Ω) in opposite direction and formed the disc speed ratio as $\Gamma = \Omega_L / \Omega_R$, where Ω_L and Ω_R are the rotational speeds of the left-hand and right-hand disc respectively. The predicted stream lines show two cells of fluid rotating in opposite direction and cancelled each other at the mid of the cavity. The significant effects of different disc speed ratios on the fluid flow behaviour were investigated at

++Correspondence Author: A. F. ABBASI E-mail address: afatah66@yahoo.com Cell # 03362572128

[b] Department of Mechanical Engineering, Shaheed Zulfiqar Ali Bhutto Campus Mehran University of Engineering and Technology, Khairpur Mirs, Sindh, Pakistan. E-mail address: sadiq.shah@manchester.ac.uk

[c], Department of Industrial Engineering & Management Mehran University of Engineering and Technology, Jamshoro, Sindh, Pakistan. E-mail address: jumanisalih@hotmail.com

[d] Department of Electrical Engineering, Mehran University of Engineering and Technology, Jamshoro, Sindh, Pakistan.

varying mass flow rates and found reasonable agreement with the measurements of (Chen *et al.*, 1997).

2. GEOMETRY AND BOUNDARY CONDITIONS

2.1 Geometry

The geometry of interest based on the experimental work of (Chen et al.,1997). The geometrical dimensions are:

s=0.046m, b=0.381m, and G=0.12

where, s, b, ri and G are the axial distance, outer radius, inlet radius and gap ratio respectively.

2.2 Boundary Conditions

At inlet, the cooling air is supposed to enter the cavity with axial uniform velocity and leave the cavity with uniform radial velocity, which verified the mass balance within the cavity. The mass flow rate and rotational Reynolds number are ranges to C_w= 4026≤ 9351 and $Re_\Theta = 1.14x10^6 \leq 1.19x10^6$ respectively.

3. TURBULENCE MODELS

Turbulence models, the low Reynolds number k-ε model and low Reynolds number second moment closure ($\overline{u_i u_j}$) have been implicated for the simulations. These turbulence models are categorized according to the modelling procedure of the Reynolds stress terms which were formed during the averaging process of the Navier-Stokes equations as mentioned (Lai and So, 1990). For the calculation of these stress terms, two approaches, isotropic eddy viscosity and non-isotropic eddy viscosity were invoked. Further more for the assessment of near wall flow; the near wall treatment was given by applying the wall damping functions between first grid point and the wall surface. Consequently, the turbulent transport quantities in the near-wall region were minimized and the boundary conditions being imposed at the wall.

3.1 Low Reynolds Number k-ε Model

These model equations are based on the isotropic eddy viscosity approach of (Morse, 1991), which were derived on the basis of gradient transport hypothesis.

$$\overline{\rho u_i u_j} = 2/3\delta_{ij}\,\rho k - \mu_T\left(\frac{\partial U_i}{\partial x_j}+\frac{\partial U_j}{\partial x_i}-2/3\delta_{ij}\nabla.\underline{V}\right) \quad (1)$$

$$\nabla.\underline{V} = \frac{\partial U}{\partial z}+\frac{\partial V}{\partial r}+\frac{V}{r} \quad (2)$$

The term ($2/3\delta_{ij}$) stands for normal stresses.

General form of the equations

$$\frac{\partial}{\partial z}(\rho U k)+\frac{1}{r}\frac{\partial}{\partial r}(r\rho V k)=\frac{\partial}{\partial z}\left[\left(\mu+\frac{\mu_T}{\sigma_k}\right)\frac{\partial k}{\partial z}\right]+\frac{1}{r}\frac{\partial}{\partial r}\left[r\left(\mu+\frac{\mu_T}{\sigma_k}\right)\frac{\partial k}{\partial r}\right]+S_k \quad (3)$$

$$\frac{\partial}{\partial z}(\rho U \varepsilon)+\frac{1}{r}\frac{\partial}{\partial r}(r\rho V \varepsilon)=\frac{\partial}{\partial z}\left[\left(\mu+\frac{\mu_T}{\sigma_\varepsilon}\right)\frac{\partial \varepsilon}{\partial z}\right]+\frac{1}{r}\frac{\partial}{\partial r}\left[r\left(\mu+\frac{\mu_T}{\sigma_\varepsilon}\right)\frac{\partial \varepsilon}{\partial r}\right]+S_\varepsilon \quad (4)$$

were the source terms S_k and S_ε see detail in reference

3.2 Low Reynolds Number Second Moment Closure

These modelling equations are based on the suggestions of (Memon , 1999) and (Lai and So,1990)in which an isotropic eddy viscosity approach is not invoked during the modelling procedure. All the turbulence quantities are calculated individually. The Reynolds-averaged mean flow governing equations for the steady turbulent flow can be written in the Cartesian tensor notation as

$$\frac{\partial}{\partial x_j}\left(\rho U_i U_j\right)=-\frac{\partial P}{\partial x_i}+\frac{\partial}{\partial x_j}\left(\mu\frac{\partial U_i}{\partial x_j}-\rho\overline{u_i u_j}\right) \quad (5)$$

where, U_i and u_i are the ith components of the mean and fluctuating velocity respectively, P is mean static pressure, ρ and μ are the fluid density and viscosity respectively. The term $\overline{u_i u_j}$ represents the six components of the Reynolds stress tensor that can be determined by the turbulence model.

This axisymmetric and steady flow equation can be written in the cylindrical- polar coordinate system and represented by the general form for a variable ϕ as

$$\frac{\partial}{\partial x}(\rho U\phi)+\frac{1}{r}\frac{\partial}{\partial r}(r\rho V\phi)=\frac{\partial}{\partial x}\left(\mu\frac{\partial\phi}{\partial x}\right)+\frac{1}{r}\frac{\partial}{\partial r}\left(r\mu\frac{\partial\phi}{\partial r}\right)+s_\phi \quad (6)$$

where the pressure gradient and the Reynolds stress tensor appearing in Equation (6) are represented by the corresponding source term s_ϕ. The net source term for the momentum equations $\phi = U, V$ and W/r in the axial, radial and tangential directions respectively, can be expressed as follows:

ms:

$$s_U=-\frac{\partial P}{\partial x}-\frac{\partial}{\partial x}\left(\rho\overline{u^2}\right)-\frac{1}{r}\frac{\partial}{\partial r}\left(r\rho\overline{uv}\right) \quad (7)$$

$$s_V=-\frac{\partial P}{\partial r}-\frac{1}{r}\frac{\partial}{\partial r}\left(r\rho\overline{v^2}\right)-\frac{\partial}{\partial x}\left(\rho\overline{uv}\right)-\mu\frac{V}{r^2}+\rho\frac{W^2}{r}+\rho\frac{\overline{w^2}}{r} \quad (8)$$

$$s_{w/r} = -\frac{\partial}{\partial x}\left(\rho r\overline{uw}\right) - \frac{1}{r}\frac{\partial}{\partial r}\left(\rho r^2\overline{vw}\right) \quad (9)$$

The governing transport equation for the Reynolds stress tensor can be expressed in Cartesian tensor as

$$\frac{\partial}{\partial x_k}\left(\rho U_k\overline{u_i u_j}\right) = \frac{\partial}{\partial x_k}\left(\mu\frac{\partial\overline{u_i u_j}}{\partial x_k}\right) + \frac{\partial}{\partial x_k}\left(-\rho\overline{u_i u_j u_k}\right) \quad (10)$$

$$-\rho\left(\overline{u_j u_k}\frac{\partial U_i}{\partial x_k} + \overline{u_i u_k}\frac{\partial U_j}{\partial x_k}\right) - \overline{\left(u_i\frac{\partial p}{\partial x_j} + u_j\frac{\partial p}{\partial x_i}\right)} - 2\mu\overline{\frac{\partial u_i}{\partial x_k}\frac{\partial u_j}{\partial x_k}}$$

or symbolically as

$$C_{ij} = D_{ij}^{v} + D_{ij}^{T} + P_{ij} + \Pi_{ij} - \varepsilon_{ij} \quad (11)$$

Term on left side is convection and right side viscous diffusion, turbulent diffusion, production by mean strain, redistribution and diffusion due to the pressure interactions and viscous dissipation of the Reynolds stresses, respectively.

4. COMPUTATIONAL PROCEDURE

The computational procedure of TEACH uses a finite volume technique (FVM) and adopts the line-by-line method based on the tri-diagonal matrix algorithm (TDMA) to solve the discretised transport equations. All the variables are solved at the main grid nodes, except the axial and radial momentum equations which solved by using the staggered grid arrangement of (Harlow and Welch, 1965). A grid arrangement of 75x92 nodes in the axial and radial directions respectively was adopted as depicted in **(Fig. 1 and 2).** This numerical method also adopts the SIMPLE algorithm of (Patankar and Spalding, 1972) to update the pressure field and correct the velocity values to satisfy the mass continuity. However, (Morse, 1991) incorporated the SIMPLEC algorithm of (Doormal and Raithby, 1984) and this same has been used in the present work. The advantages of the SIMPLEC algorithm over the SIMPLE and its extended version SIMPLER introduced by (Patankar, 1980). All the variables of mean and fluctuating quantities are discretised through the HYBRID (Spalding, 1972]) and HOUS (Castro and Jones, 1987) interpolation schemes. For further detail see references, (Memon, 1995), (Morse, 1991) (Abbasi *et al.,* 2012).

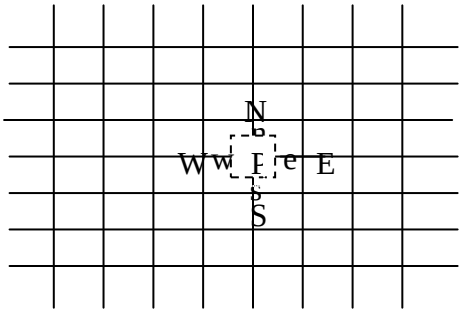

Fig. 1. Staggered grid arrangements

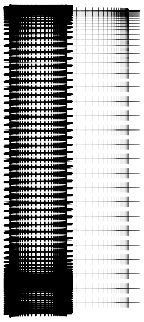

Fig. 2. Non-uniform grid

5. DISCUSSION OF SIMULATED RESULTS

5.1 Simulated flow structure

Fig. 3 shows the simulated stream lines of two models for the rotational Reynolds number, $R_{e\Theta}$= $1.19x10^6$ and mass flow rate, C_w= 9351 at disc speed ratio of Γ= - 1. The simulated stream lines of the fluid formed from source region of the cavity and recirculated in outer region of the cavity. Result of that two cores of the fluid are formed in the outer region of cavity. These recirculation cores of fluid developed the double cell structure, which signifies the effects of counter rotation of the two discs. Fluid flow behaviour of these cells shows that the laminar flow along the disc surface and transitional flow in the centre of cavity, which attributed the effects of reverse flow in the mid of cavity. These recirculation cells were cancelled each other at a point known as a stagnation point. The same flow behavior was illustrated in the work of (Dijkstra and van Heijst, 1983) , (Kilic et al.,2003), (Gan and Macgregor,1995) and (Abbasi *et al.,* 2012) .

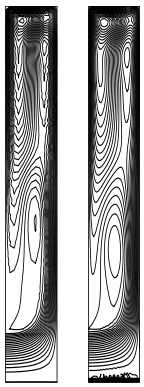

$\overline{u_i u_j}$ k - ε

Fig.3. Comparison of computed stream lines for $Re_\Theta = 1.19x10^6$ and

5.2 Computed velocity profiles

Fig. 4a shows the axial variation of radial and tangential velocity component for Re_Θ = $1.14x10^6$ and C_w= 4026 at two radial locations, r/b=0.7,0.85. likewise, radial velocity profile along the discs show the laminar boundary layers and reverse velocity in the

centre (z/s = ½) shear region, which signifies the fluid flow behaviour of recirculating cores **(Fig.3).**This reverse flow behaviour of the fluid formed the negative profile of the velocity which attained the maximum level in the centre. The same velocity behavior has been observed for the tangential velocity profile, which varies between the two discs space and attained zero level in the centre of the disc space. **(Fig. 4b)** also shows the comparison of two models at higher radial location r/b=0.85. At this higher radial location no any significant change in the results except both the boundary layers, which are illustrated the lower level of velocity profiles on both sides of the discs. Decrease in the boundary layers profiles attributed that the reversed flow obtained at higher radial location than the lower one. The comparison of two models with experimental data for radial velocity shows the closer agreement except at the mid plane region where Reynolds stress ($\overline{u_i u_j}$) model has the better agreement than that of the k-ε model. **(Fig. 5a-b)** presents the comparison of two models with measurements for the radial and tangential velocity components for 4% higher rotational Reynolds number, Re_Θ=1.19x10^6,and 57% higher mass flow rate, Cw=9351 than the previous case, at two radial locations, r/b=0.8 and 0.85. The comparison of the radial and tangential velocity components at higher radial location r/b=0.8 shows the $\overline{u_i u_j}$ model shows the closer agreement with the measurements in all flow regions than that of the k-ε model, which is underestimated on the left side boundary layer and overestimated in the recirculating core region. The predicted tangential velocity profiles of both the models show the good agreement between the measurement. For the highest radial location r/b= 0.85, the comparison between prediction and measurement shows that both the models showed the significant difference on left side boundary layer, where both models are underpredicted. The identical trends of discrepancy also observed at lower radial location. At the midplane turbulent region both models were also overpredicted. However, the comparison of tangential velocity profiles of both the models are again show a good agreement with the measurements.

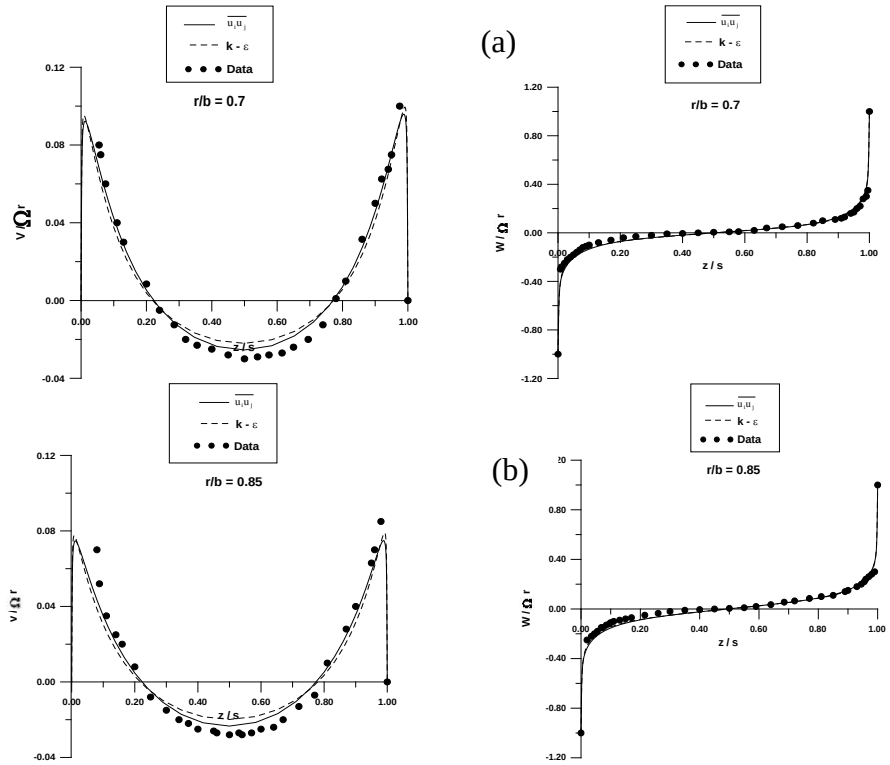

Fig.4: Comparison between radial and tangential velocity profiles for Re_Θ = 1.14x10^6, Cw = 4026 and Γ = -1, at radial location

(a) r/b = 0.7, (b) r/b = 0.85

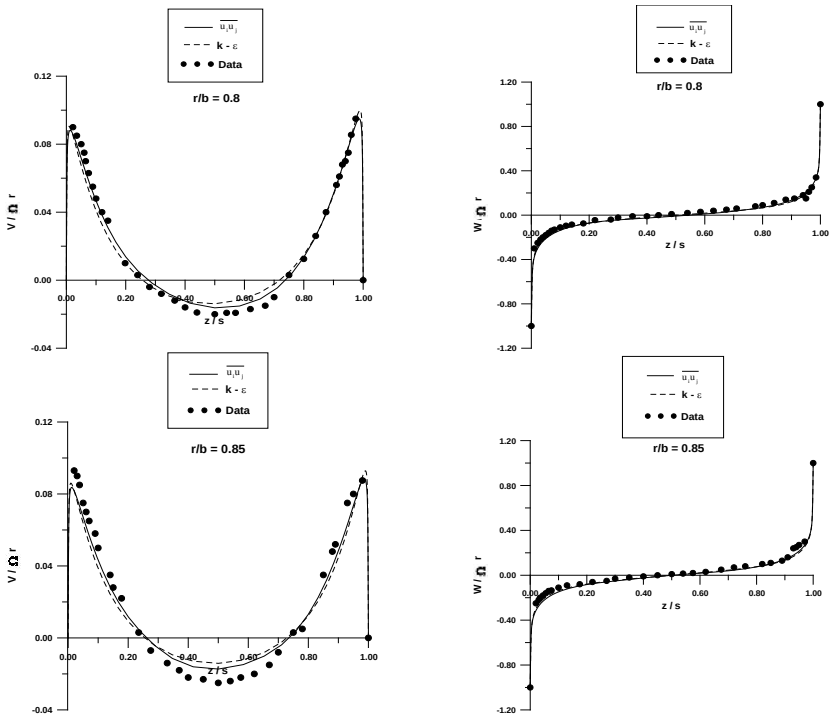

Fig.5: Comparison between radial and tangential velocity profiles for $Re_\Theta = 1.19x10^6$, Cw = 9351 and Γ = -1, at radial location (a) r/b = 0.8, (b) r/b = 0.85

5.3 Computed moment coefficient

Table 1: Comparison of computed moment coefficient for $Re_\Theta = 1.14x10^6 \leq 1.14x10^6$, $C_w = 4026 \leq 9351$ at Γ =-1

Re_Θ	C_w	$\overline{u_i u_j}$ model $C_m \times 10^3$	k-ε model $C_m \times 10^3$	Difference
1.14×10^6	4026	5.057	4.174	17%
1.19×10^6	*9351*	*5.1*	*4.23*	*17%*

Table 1 presents the comparison of computed moment coefficient for two models for the range of $Re_\Theta = 1.14x10^6 \leq 1.14x10^6$ and $C_w = 4026 \leq 9351$. It can be seen from the table, the computed moment coefficient of two models show difference of 17%. This difference increased monotonically by for 4% higher rotational Reynolds number ($Re_\Theta = 1.14x10^6$) and 57% higher mass flow rate ($C_w = 9351$). This percentage difference in results shows the consistency of models, which can be maintained for higher operating conditions.

6. CONCLUSIONS

Modelling and simulations of contra-rotating discs system have been carried for the range of rotational Reynolds number, $Re_\Theta = 1.14x10^6 \leq 1.14x10^6$ and mass flow rate, $C_w = 4026 \leq 9351$at fixed value of disc speed ratio of $\Gamma = -1$. The computed flow structure between two contra rotating discs illustrated the two cells of fluid, which were rotated in opposite direction. Due to recirculating behaviour of the fluid cells, both cancelled each other in the centre of the cavity. The point where these cells cancelled each other is known as stagnation point. The location of this stagnant point can vary for different disc speed ratios. The computed velocity profiles of two models signified the same trend of counter-rotation of fluid cells. The radial velocity profiles show negative value of velocity in the centre of the cavity, which attributed the recirculation of the fluid in the mid plane region. The tangential velocity profile also showed the consistency with the flow behavior and radial velocity profile. The computed moment coefficient of two models showed the 17% variation in

results of two models, this difference was maintained for higher operating conditions. These results attributed that both models can be applied confidently for complex flow situation. Overall comparison of results showed that Reynolds stress model depicted the better with the measurements of (Chen *et al.,* 1997) than that of the k-ε model.

REFERENCES:

Abbasi, A. F.,(2013) Stressing of turbine disc for isothermal and non-isothermal rotating disc flows, D.Phil. Thesis, Mehran University of Engineering And Technology.

Abbasi, A. F., M. D. Memon and A. Baloch, (2012) Numerical Prediction of Closed Contra-Rotating Disc Flows. Mehran University Research Journal of Engineering & Technology 31(04): 683-696.

Castro, I. P. and J. M. Jones, (1987) Studies in Numerical Computations of Recirculating Flows. Int. J. Num. Methods in Fluids 7: 793-802.

Chen, X., X. Gan, and J. M. Owen, (1997) Heat transfer from air-cooled contra-rotating discs. J. Turbomachinery 117: 61-67.

Dijkstra D. and G.J.F. vanHeijst, (1983) The Flow Between two Finite Rotating Discs Enclosed By ACylinder. Journal of Fluid Mechanics 128:123-154.

Gan, X.P. and S.A. Macgregor, (1995) Experimental Study of the Flow in the Cavity Between Rotating Discs. Experimental Thermal Fluid Science 10: 379-387.

Gan, X., M. Kilic and J.M. Owen, (1995) Flow between Contra-rotating Discs. J. Turbomachinery 119: 298-305.

Gan, X., M. Kilic, J. M. Owen (1994) Superposed flow between two discs contra-rotating at differential speeds, Int. J. Heat Fluid Flow. 15: 438-446.

Harlow, F. H. and J. E. Welch, (1965) Numerical Calculation of Time-Dependent Viscous Incompressible Flow of Fluid with Free Surface. Physics of Fluids 8: 2182-2189.

Hill, R. W. and K.S. Ball, (1997) Chebyshev Collocation Analysis of Axisymmetric Flow and Heat Transfer between Counter-Rotating Discs, ASME, Journal of Fluids Engineering 119: 940-947.

Hill, R. W. Hill and K. S. Ball, (1999) Direct Numerical Simulations of Turbulent Forced Convection between Counter-Rotating Discs. International Journal of Heat and Fluid Flow. 20: 208-221.

Kilic, M., X. Gan and J.M. Owen, (1994) Transitional Flow between Contra-Rotating Discs. Journal of Fluid Mechanics 281: 119-135.

Kilic, M., X. Gan, Owen, J. M, (1995) Turbulence flow between two discs contra-rotating at different speeds. J. of Turbomchinery 118: 408-413.

Kilic M. and J. M. Owen, (2003) Computation of flow between two discs rotating at different speeds. J. of turbomachinery. 125: 394-400.

Lai, Y. G. and R. M. C. So, (1990) On near-wall turbulent flow modelling. J. Fluid Mech. 221641-673.

Morse, A. P., (1988) Numerical prediction of turbulent flow in a rotating cavities. J. Turbomachinery 110: 202-211.

Morse, A. P. (1991) Application of a low Reynolds number k-e turbulence model to high-speed rotating cavity flows, J. of Turbomachinery 113: 98-105.

Memon, M. D., (1995) Numerical modelling and prediction of fluid flow and heat transfer in rotating disc geometries, D.Phil. Thesis, University of Sussex.

Memon, M. D. (1999) Development of the low Reynolds Number Second Moment Closure. Mehran University Research J. of Engineering & Technology 18: 33-37.

Patankar, S. V. and D.B.Spalding, (1972) A calculation procedure for heat, mass and momentum transfer in three-dimensional parabolic flow. Int. J. Heat and Mass Transfer15: 1787-1806.

Patankar, S. V. (1980) Numerical heat transfer and fluid flow. McGraw-Hill, New York.

Remi M. (2014) Recent progress in the development of the Elliptic Blending, Reynolds-stress model. International Journal of Heat and Fluid Flow 48:43-51.

Soong, C.Y., C.C. Wu, T. P. Liu, (2003) Flow structure between two co-axial discs rotating,independently. Experimental Thermal and Fluid Science 27: 295-313.

Spalding, D. B. (1972) A Novel Finite-Difference Formulation for Differential Expression Involving Both First and Second Derivatives. International Journal of Numerical Methods Engineering 4: 551-559.

Van Doormal, J. P. and G. D. Raithby, (1984) Enhancement of the SIMPLE method for predicting incompressible fluid flow. Num. Heat Transfer 7: 147-163